ACS Sustainable Chemistry & Engineering

Research Article

pubs.acs.org/journal/ascecg

Sunlight Induced Synthesis of Reversible and Reusable Biocapped Nanoparticles for Metal Ion Detection and SERS Studies

Somasundaram Kaviya and Edamana Prasad*

Department of Chemistry, Indian Institute of Technology Madras, Chennai-600 036, India

Supporting Information

ABSTRACT: The present work describes an eco-friendly synthesis of silver and gold nanoparticles using an aqueous extract of the bone powder of a dry marine organism (seahorse), which acts both as a reducing as well as stabilizing agent. The novel photoinduced formation of the nanoparticles (NPs) was characterized by UV−vis absorption, dynamic light scattering, scanning electron microscopy (SEM), and transmission electron microscopy (TEM) experiments. The role of pH on the feasibility of nanoparticle formation has been investigated. The results suggest that photoinduced electron transfer from the amino acids present in the bone extract is responsible for the reduction of the nanoparticle precursors. The as-synthesized nanoparticles have been utilized as "naked eye" sensors for the detection of multiple ions (Cu^{2+}, Cr^{3+}, V^{4+}, and UO_2^{2+}) at *micromolar* concentration of the analytes. Furthermore, the NPs were found to enhance the surface Raman peaks from dye molecule (rhodamine 6G) at *nanomolar* concentration of the analyte. More significantly, a novel and efficient sunlight induced reversible aggregation pathway for the as-synthesized nanoparticles has been demonstrated.

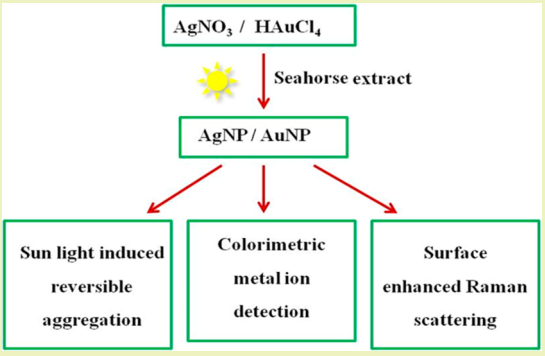

KEYWORDS: *Metal ion sensor, Nanoparticles, Naked eye detection, Seahorse, Reversible aggregation, SER spectroscopy*

INTRODUCTION

Recent years have witnessed a wide range of physical,[1] chemical,[2] and biological[3] methods of synthesizing nanomaterials with controlled size, shape, and aspect ratios. The functional properties of nanoparticles strongly depend on the size and shape of the metal nanoparticles formed.[4,5] Among the various methods of nanoparticle preparation, reduction of metal ions using suitable reducing agents has been found to be the most common pathway. In this protocol, the capping agent, which reduces and/or stabilizes the metal nanoparticle in the solution, plays a key role in the overall synthetic scheme. The capping and reducing agents used in the chemical synthetic approaches are toxic, costly, and, oftentimes, not ecofriendly. Hence, biological capping agents for synthesizing/stabilizing nanoparticles have emerged as an attractive alternate. Synthesis of nanoparticles using sunlight[6,7] and stabilizing them by biological capping agents from natural resources such as microorganisms (e.g., alga, fungi, etc.),[8,9] and plant extract[3,10,11] provide great advancement over existing chemical and physical methods since they are renewable, cost-effective, and ecofriendly.

Seahorse is a fish which has been mainly found in shallow tropical and temperate water throughout the world. The extract of the seahorse bone from the dry seahorse has been used in traditional Chinese medicine (TCM).[12] There are five different types of seahorse, classified according to their skeletal characteristics: *Hippocampus kuda*, *Hippocampus spinnossimus*, *Hippocampus fuscus*, *Hippocampus kellogi*, and *Hippocampus trimaculatus*.[12] Herein, we report a sunlight induced green synthetic route for AgNPs and AuNPs in presence of aqueous extract of *dry bone powder* of seahorse. Subsequently, these nanoparticles have been used for detecting multianalytes such as Cu^{2+}, Cr^{3+}, V^{4+}, and UO_2^{2+} ions at micromolar concentrations in aqueous conditions. The detection is based on color change, which can be observed by naked eye.

Detection of these toxic metal ions is vital since the continuous exposure of them causes serious respiratory track problems, neurodegenerative issues,[13] genotoxic effect,[14] and kidney deterioration.[15] While NPs stabilized by different synthetic capping agents have been previously utilized as colorimetric sensors for the above-mentioned toxic metal ions,[16−27] biological capping agents from single extract, which can detect all of them together, has not been reported till date. The attractive part of the multidetection is that the process is simple, cost-effective, and time saving compared to single-analyte detection.[21]

Moreover, the stabilized metal nanoparticles were used to generate surface enhanced Raman scattering signals for a dye molecule (Rhodamine 6G), at nanomolar concentration of the analyte. The biologically capped NPs were highly stable, and the sample took more than twelve months to exhibit any sign of aggregation. Furthermore, the aggregation was completely

Received: October 4, 2013
Revised: December 5, 2013
Published: December 26, 2013

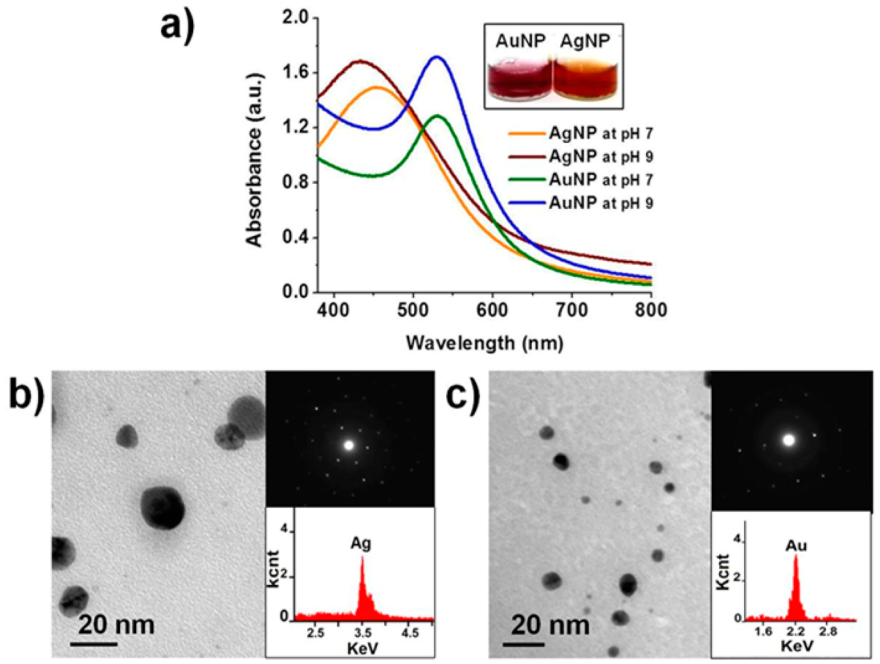

Figure 1. (a) UV−vis absorption spectra of Ag and AuNPs stabilized by dry seahorse extract at two different pH (7 and 9) and the corresponding photographs (inset). (b and c) TEM images of Ag and AuNPs, respectively. The insets in b and c are the corresponding SAED pattern (above) and EDAX profile (below).

reversible upon exposing the sample to sunlight for a few minutes.

EXPERIMENTAL SECTION

Materials and Synthesis of Nanoparticles. All chemicals were obtained from Aldrich (USA) and used as received without further purification. Ultrapure water from Direct Q Millipore was used for the experiments. The dry seahorse was milled using a normal grinder in the laboratory and the powder (1.0 g) was boiled in ultrapure water (50 mL) for 15 min. After filtration, the clear extract was stored at refrigerator for further use. The extract (3 mL) was added to an aqueous solution of silver nitrate (30 mL, 10^{-4} M) and chloroauric acid (30 mL, 10^{-4} M). The reaction vessel was exposed to sunlight, without stirring, for 1.0 h for the preparation of AuNP and 0.50 h for the preparation of AgNP.

Colorimetric Detection of Metal Ions and SERS Study. The aqueous solution of metal salts (10^{-1}−10^{-6} M), rhodamine 6G (10^{-9} M), ethylenediaminetetraacetic acid (EDTA) (10^{-2} M), and NaOH (0.01M) were prepared. The metal salt (~200 μL) was added to the NPs solution (200 μL) in aqueous medium and pH was adjusted by adding NaOH solution. The color changes for the specific metal ions were observed within seconds. For SERS studies, rhodamine 6G (30 μL) was added to the NPs solution (10 μL) in water (~200 μL). The experiments were carried out at room temperature. The photographs were taken with Canon A3200 IS digital camera.

Characterization Techniques. UV−visible spectroscopic studies were recorded by JASCO V660 spectrometer. The IR spectra have been recorded using Perkin-Elmer FT-IR spectrometer. Photoluminescence measurements were carried out by Fluoromax-4 (HORIBA Jobin Yuvin) spectrofluorometer. Zeta potential and particle size measurements were carried out using zeta sizer (Malvern instrument). X-ray diffraction (XRD) analysis is performed by Bruker D8 advance powder X-ray diffractometer using Cu Kα radiation. The Raman measurements were conducted with a WITEC Alpha 300R laser Raman microscope equipped with a 532 nm laser of 2 μm spot size in diameter for excitation. The size and morphology of the Ag and Au NPs were examined using scanning electron microscopy (SEM) (Quanta FEG 200) and transmission electron microscopy (TEM) (Philips Tecnai 12) operated at 120 kV. Energy dispersive X-ray spectroscopy (EDAX) and selective area electron diffraction (SAED) analysis were performed by TEM, equipped with an EDAX and SAED attachment.

RESULTS AND DISCUSSION

Characterization of the NPs. Bone extract of dry marine organisms provides an excellent source of biocompatible molecules, which are potentially capable to act as capping agents for metal nanoparticles or clusters due to the abundance of proteins and essential amino acids present in the extract.[28] In the presence of sun light, addition of the dry seahorse extract to $AgNO_3$ and $HAuCl_4$ solutions (10^{-4} M) results in a rapid color formation. The silver nitrate solution turned to yellowish brown and chloroauric acid solution became pink in color, indicating the formation of silver and gold NPs in the respective systems.[9,29] Interestingly, no color changes have been observed upon mixing the seahorse extract and NP precursors, upon heating or stirring *under dark conditions*. The surface plasmon resonance (SPR) peaks for gold and silver NPs occur at 450 and 520 nm, respectively (Figure S1, Supporting Information). The formation of nanoparticles was initially monitored with UV−vis spectra (Figure 1a) by exposing the reaction mixture in the presence of sun light at different time intervals ranging from 1 min to 1 h. While the absorption maxima of the NPs remain identical for experiments with various irradiation times, the intensity of the peak increases till 4 min of irradiation for the case of silver NP. For gold NP, the plasmon peak was visible after 5 min of irradiation and the intensity of the peak increases up to 26 min (Figure S1, Supporting Information).

The formation of Ag and Au NPs was confirmed by transmission electron microscopy (TEM). The results suggest that the particles are spherical in shape. The size of the particle was 20 ± 5 nm for AgNP and 10 ± 2 nm for AuNP (Figure 1b and c). Selected area electron diffraction patterns (SAED) of the NPs correspond to (111), (200), (220), and (311) Bragg's reflection based on the fcc structure of Ag and AuNPs. The

dx.doi.org/10.1021/sc400404m | ACS Sustainable Chem. Eng. 2014, 2, 699−705

presence of elemental silver and gold can be observed in the graphs obtained from EDAX analysis, which also supports the SAED results (Figure 1b and c inset). Moreover, XRD patterns of the sample indicate the peaks corresponding to identical fcc structures obtained from SAED analysis (Figure S2, Supporting Information). The TEM images suggest that NPs are stabilized and not aggregated in presence of the biocapping agent at pH 7.

Effect of pH. Next, the effect of pH on the formation of NP has been studied. There is no formation of NPs under acidic conditions. The UV−vis absorption spectra of surface plasmon absorption of the nano silver and gold are given in Figure 1a and Figure S3 (Supporting Information). It was noted that SPR peak intensity and bandwidth are influenced by varying the pH. There is no change in the absorption maxima of the NPs, but the intensity of the peak slightly increases upon changing the pH of the medium from 7 to 9 (Figure 1a orange and brown traces for AgNP; green and blue traces for AuNP).[30] As the pH becomes more basic, the intensity of the peak is decreased as well as the peak width was broadened.

The results indicate that photoinduced electron transfer between amines (present in the amino acids in the biological capping agent) and the metal ions could be a likely mechanism for the NP formation. The shift in the absorption bands of the NPs as a function of pH indicates aggregation at basic pH, and the spectral broadening indicates the anisotropic nature of the aggregation.[31]

Dynamic Light Scattering Study. Dynamic light scattering study also substantiates the results from pH study, indicating that the size of the NPs has increased at basic pH (Table S1, Supporting Information). The zeta potential study of the NPs showed that the surface charge becomes highly negative at basic pH values, presumably due to the aggregated biocapping ligands on the NPs. The large values (∼−30 mV) of the zeta potential indicate that the aggregates formed are stable and the system does not lead to precipitation or coagulation.

Mechanistic Aspects. The main components of the dry seahorse extract are phthalate derivatives, antioxidants,[32] and essential amino acids.[28] It has also been reported that arginine, aspartic acid, glutamic acid, alanine, and glycine are the major amino acids present in the *Hippocampus kuda*.[28] The FT-IR spectroscopic analysis of seahorse extract suggests that the system contains amine groups, carbonyl, and alkyl groups (Figure S4a, Supporting Information). For example, the absorption band at 3360 cm^{-1} is due to N−H stretching vibrations of amines. The bands at 2945, 2833, and 1449 cm^{-1} are attributed to C−H stretching vibrations and the band at 1657 cm^{-1} is due to amide C═O stretching vibration.[33] The UV−vis absorption spectra of the aqueous extract contain a peak at 280 nm, which is due to $\pi-\pi^*$ transition of aromatic residues present in the protein (Figure S4b, Supporting Information).[34] Fluorescence spectra of the seahorse extract was recorded at 445 nm, which is most likely originated from a tryptophan residue (Figure S5a, Supporting Information). While tryptophan emission usually appear in the blue region of the spectrum, significant red-shifted emission from tryptophan has been reported at varied environments.[35,36]

The fact that the reduction of the metal ions occurs only in presence of sunlight suggest that the mechanism of the nanoparticle formation might include an excited state electron transfer from the amines present in the amino acids to Ag or Au ions.[37,38] The photogenerated NPs can be stabilized by the excess amount of capping agent present in the system. This is further evident from the complete quenching of the intrinsic emission from the extract, upon formation of NPs in the system (Figure S5b and c, Supporting Information). The fluorescence quenching is attributed to the self-quenching mechanism under the aggregated conditions. pH dependent study also substantiated the photoinduced electron transfer since no NP formation is observed at pH 2, due to the protonation of nitrogen atoms in the amino acids in the system.

Detection of Metal Ions by Ag and AuNPs. The results from the previous experiments suggest that the functional groups in the seahorse extract are anchored on the surface of the nanoparticles and stabilize them in the medium. We hypothesize that the functional groups in the extract can also complex with other metal ions present in the system, and such metal−ligand interactions can lead to NP aggregation. It is highly likely that such aggregation will lead to inter plasmonic oscillations by NP and associated color changes. Sensing through observable color variations in presence of analytes are highly desirable because such detection events can be visualized by naked eye, provided the sensitivity of the system is very high.

The NPs, which are stabilized by the seahorse extract, were treated with a series of metal ions (19 metal ions for AgNP and 16 metal ions for AuNP; see the Supporting Information for more details). Among the pool of the metal ions, the NPs exhibit a color change only for Cu^{2+}, Cr^{3+}, V^{4+}, and UO_2^{2+} at *micromolar* concentration of the analytes. As the metal ions mentioned above are toxic and cause environmental and health hazards,[13−15] we have decided to carry out a systematic study of the detection of the metal ions using the seahorse stabilized Ag and Au NPs.

The stabilized NPs have been treated with a series of different metal ions (0.01 M; Figures S6 and S7, Supporting Information). Addition of a solution of V^{4+} ions to seahorse stabilized AgNPs leads to the formation of a black color precipitate (Figure 2a inset). At pH 7, micromolar concentration of V^{4+} ion generates a black color formation along with a clear spectral broadening of AgNP from 400 to 700 nm. Upon increasing the concentration of V^{4+}, enhanced aggregation and precipitation of NPs has been observed. The TEM analysis of the precipitate indicates the formation of AgNPs, with dendritic type morphology (Figure 2b).

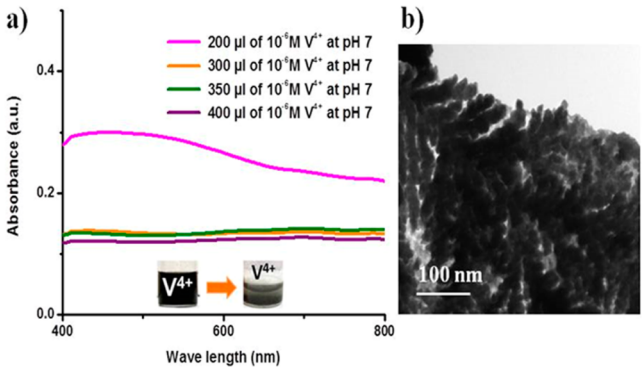

Figure 2. (a) UV−vis absorption spectra of AgNP with the addition of different aliquots of V^{4+} [μM] at pH 7 and (b) TEM image of black color aggregates.

Conversely, stabilized AuNPs exhibit *green* color upon addition of V^{4+} metal ions at pH 7. While AgNPs were sensitive only toward V^{4+} ions, the AuNPs were sensitive toward Cu^{2+}, Cr^{3+}, and UO_2^{2+}, in addition to V^{4+} ions, at

dx.doi.org/10.1021/sc400404m | ACS Sustainable Chem. Eng. 2014, 2, 699−705

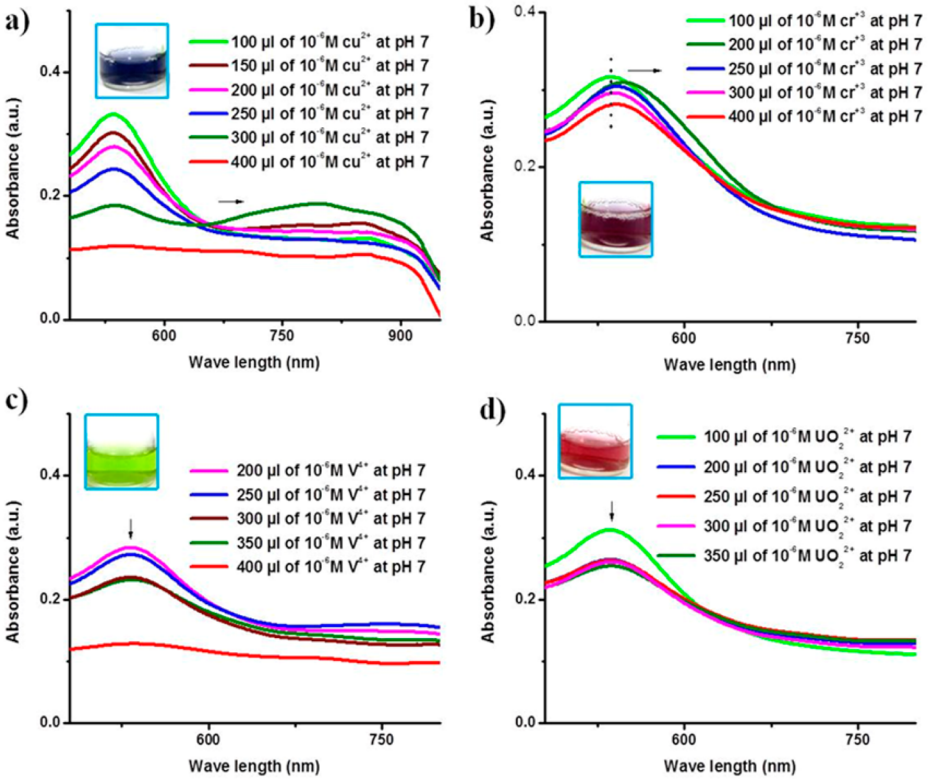

Figure 3. UV−vis absorption spectra shows the detection of (a) Cu^{2+}, (b) Cr^{3+}, (c) V^{4+}, and UO_2^{2+} by AuNPs at pH 7.

micromolar concentrations. The pink colored AuNP solution was turned to blue, violet, and red in the presence of micromolar concentrations of Cu^{2+}, Cr^{3+}, and UO_2^{2+}, respectively. The molar extinction coefficient of AuNPs solution is decreased in presence of copper ions with the formation of an additional broad absorption band from 700 to 1000 nm (Figure 3a). This suggests that presence of the metal ion enhanced the aggregation propensity of AuNPs in the system, leading to interplasmonic coupling to generate the color difference.[16,39,40]

While the addition of a micromolar concentration of Cu^{2+} to AuNP produce blue color, addition of identical concentration of Cr^{3+} gives violet color and the SPR peak of AuNP shifts to 560 nm (Figure 3b). The presence of V^{4+} ions provide a green color with the peak shift to 550 nm along with a longitudinal band at 750 nm (Figure 3c). The presence of UO_2^{2+} shifts the SPR peak with significant aggregation of NPs (Figure 3d). The TEM and SEM images of the AuNP aggregates due to the addition of the above analytes in micromolar concentration are shown in Figure S8, Supporting Information. The results from the TEM and SEM analysis indicate that the NPs are aggregated, which corroborates our hypothesis that the interaction between the capping agents of NPs and the analyte results in bringing the NPs close to each other. Under such conditions, distinct colors are generated due to the corresponding plasmon oscillations. The color changes obtained in presence of various metal ions indicate that the aggregation propensity of the seahorse capped NPs is highly sensitive toward respective metal ions.

Effect of Counterions and Chelating Agent. The AuNP mediated metal detection has been conducted in the presence of various counterions of the metal salts, and the results suggest that the counterions have negligible effect on the detection mechanism (Figure S9, Supporting Information). Control experiments have been performed with the extract alone and no color change has been observed with the addition of the analyte (Figure S10, Supporting Information). Further, we have added metal ion (Cu^{2+}, Cr^{3+}, UO_2^{2+}, and V^{4+}) solutions into $HAuCl_4$ and $AgNO_3$ separately and noticed that the color is changed only in the presence of NPs (Figure S11, Supporting Information).

In addition, we have studied the NP-metal ion interaction in the presence of metal ion chelators such as EDTA (0.01 M). It is found that the binding between the biocapping agent and the metal ion is partially reversible in presence of EDTA. It has been observed that increased reversible binding occurs at relatively higher metal ion concentration, which is due to the complex formation between the loosely bound metal ions and EDTA (Figures S12 and S13, Supporting Information). We have carried out the interference studies of Ag and Au NP with other metal ions, in presence of Cu^{2+}, Cr^{3+}, V^{4+}, and UO_2^{2+}. The results show that there were no color changes with the addition of other metal ions along with the analytes (Figures S14−16, Supporting Information). Interference studies between the analytes (Cu^{2+}, Cr^{3+}, V^{4+}, and UO_2^{2+} ions) suggests that the Au NPs are more sensitive toward chromium and uranium salts (Figures S17 and S18, Supporting Information).

Reversible Aggregation of NPs. We have examined the stability of the NP for 12 months. After a year, the nanoparticles form aggregates which were deposited at the bottom of the container. This is not unusual as the intermolecular H-bonding between the functional groups present in the protein molecule bound to the adjacent NPs leads to slow coagulation.[41] The deaggregation process of NP is usually difficult because of the formation of larger and insoluble materials in the system.[42] There are three general approaches in

dx.doi.org/10.1021/sc400404m | ACS Sustainable Chem. Eng. 2014, 2, 699−705

the literature to achieve reversible NPs: addition of linker molecules,[43] changing pH,[44] and changing temperature[45] of the medium. Initially, we attempted to study the effect of sonication, heat, and pH on the rate of disaggregation. However, the results suggest that change in any of these parameters does not lead to deaggregation (Figures S19 and S20, Supporting Information). We then attempted an alternate procedure for deaggregation of the biocapped NPs through exposing the aggregate to sunlight. Upon shining sunlight on the AuNP aggregates for 2 *min*, the solution regained the original color of the NPs at the initial stage of preparation. Time dependent UV−vis absorption spectra and TEM analysis also suggest that the size of the regenerated NPs is comparable with their initial size (Figure 4). In the case of AgNPs, time

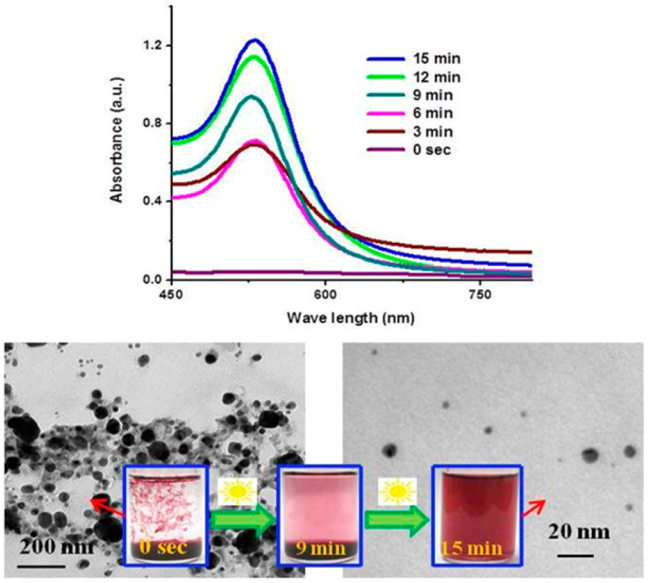

Figure 4. (a) UV−vis spectra of reversible aggregation of AuNPs in the presence of sunlight at different time intervals; (b) corresponding TEM images of the photograph in the inset.

required for reversible aggregation was more (~20 min) and remain incomplete relative to AuNP (Figure S21, Supporting Information). While more experiments have to be performed to understand the minute mechanistic aspects of the sunlight induced novel reversible aggregation pathway of AuNP, the role of photoinduced process generating alike charges in the excited state and thereby creating repulsion among the capped NPs is assumed to be the underlying reason for the disaggregation mechanism.

SERS Study. In literature, SERS of rhodamine 6G (10^{-9} M) was studied in presence of silver and gold nanoparticles, where the NPs are synthesized by chemical reduction methods.[46−48] In such cases, chemical addition method or coating method has been chosen to make the NP aggregate SERS active.[46−49] Since the biocapped NPs form stable aggregates in presence of suitable metal ions, we hypothesized that the system may generate hot-spots at the NP junctions of the aggregates.[49] In order to examine the hypothesis, surface enhanced Raman signals (SERS) has been measured from rhodamine 6G in the presence and absence of the NPs. The NPs form aggregate in presence of rhodamine 6G as well, which was evident from the UV−vis spectra (Figure S22, Supporting Information). The hot-spot formation has also been clearly observed in the case of AgNPs from confocal laser Raman microscopic image (Figure 5a). The surface enhanced Raman scattering (SERS) signals of

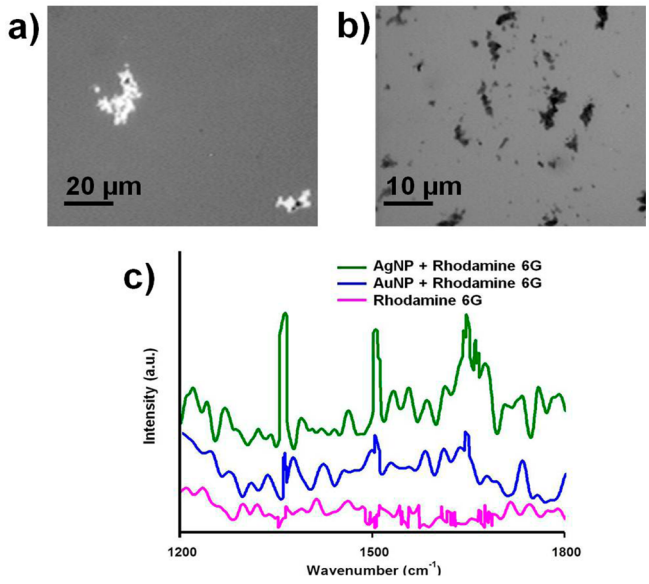

Figure 5. (a and b) Confocal laser Raman microscopic image of Ag and AuNPs in the presence of rhodamine 6G (10^{-9} M;, (c) surface enhanced Raman signals of Ag and AuNPs in the presence of rhodamine 6G (10^{-9} M).

rhodamine 6G (1360, 1504, and 1644 cm^{-1})[50] have been observed with both Ag and AuNPs (Figure 5c). It is noteworthy here that the SERS signals of rhodamine 6G have been enhanced even at extreme dilute conditions of the analyte (10^{-9} M).

In conclusion, we present a greener approach of synthesizing Ag/AuNPs, in the presence of sunlight. The NPs are water-soluble and highly stable. The as-synthesized NPs were able to aggregate in a controlled fashion in presence of selected toxic metal ions, leading to multianalyte detection of the metal ions by naked-eye at micromolar concentration of the analyte. The biocapped NPs have been further utilized for SERS of rhodamine 6G at nanomolar concentration range of the dye. A novel sunlight induced reversible aggregation pathway has been observed for the stabilized NPs. The effect of the novel biocapped Au and AgNPs on biomedical application is currently underway in our laboratory and the result will be published in due course.

■ ASSOCIATED CONTENT

Ⓢ Supporting Information

Figures for the formation of NPs at different time intervals and pH, counterion effect, interference studies, reversible aggregation studies, and table for zeta potential and size of the NPs. This material is available free of charge via the Internet at http://pubs.acs.org.

■ AUTHOR INFORMATION

Corresponding Author

*E-mail: pre@iitm.ac.in. Fax: (+) 91-44-2257-4202.

Notes

The authors declare no competing financial interest.

■ ACKNOWLEDGMENTS

S.K. thanks for the INSPIRE fellowship from DST, Govt. of India. We thank the financial support from DST Nano Mission {ref. No. SR/NM/MS-115/2010 (G)}. We thank SAIF, IITM, for FT-IR and Dr. Ramaprabu, Physics department, IITM, for providing confocal laser Raman spectrometer facility.

■ REFERENCES

(1) Jang, D.; Kim, D. Synthesis of nanoparticles by pulsed laser ablation of consolidated metal microparticles. *Appl. Phys. A: Mater. Sci. Process.* **2004**, *79*, 1985−1988.

(2) Lu, L.; Kobayashi, A.; Tawa, K.; Ozaki, Y. Silver Nanoplates with Special Shapes: Controlled Synthesis and Their Surface Plasmon Resonance and Surface-Enhanced Raman Scattering Properties. *Chem. Mater.* **2006**, *18*, 4894−4901.

(3) Akhtar, M. S.; Panwar, J.; Yun, Y. S. Biogenic Synthesis of Metallic Nanoparticles by Plant Extract. *ACS Sustainable Chem. Eng.* **2013**, *1*, 591−602.

(4) Huschka, R.; Zuloage, J.; Knight, M. W.; Brown, L. V.; Nordlander, P.; Halas, N. J. Light-Induced Release of DNA from Gold Nanoparticles: Nanoshells and Nanorodes. *J. Am. Chem. Soc.* **2011**, *133*, 12247−12255.

(5) Duan, C.; Cui, H.; Zhang, Z.; Liu, B.; Guo, J.; Wang, W. Size-Dependent Inhibition and Enhancement by Gold Nanoparticles of Luminol-Ferricyanide Chemiluminescence. *J. Phys. Chem. C* **2007**, *111*, 4561−4566.

(6) Jin, R.; Cao, Y.; Mirkin, C. A.; Kelly, K. L.; Schatz, G. C.; Zheng, J. G. Photoinduced Conversion of Silver Nanospheres to Nanoprisms. *Science* **2001**, *294*, 1901−1903.

(7) Yang, L. B.; Chen, G.; Wang, J.; Wang, T. T; Li, M.; Liu, J. Sunlight-induced formation of silver-gold bimetallic nanostructures on DNA template for highly active surface enhanced Raman scattering substrates and application in TNT/tumor marker detection. *J. Mater. Chem.* **2009**, *19*, 6849−6856.

(8) Hebbalalu, D.; Lalley, J.; Nadagouda, M. N.; Varma, R. S. Greener Techniques for the Synthesis of Silver Nanoparticles Using Plant Extracts, Enzymes, Bacteria, Biodegradable Polymers, and Microwaves. *ACS Sustainable Chem. Eng.* **2013**, *1*, 703−712.

(9) Mukherjee, P.; Ahmad, A.; Mandal, D.; Senapati, S.; Sainkar, S. R.; Khan, M. I.; Parishcha, R.; Ajaykumar, P. V.; Alam, M.; Kumar, R.; Sastry, M. Fungus-Mediated Synthesis of Silver Nanoparticles and Their Immobilization in the Mycelial Matrix: A Novel Biological Apporach to Nanoparticle Synthesis. *Nano Lett.* **2001**, *1*, 515−519.

(10) Njagi, E. C.; Huang, H.; Stafford, L.; Genuino, H.; Galindo, H. M.; Collins, J. B.; Hoag, G. E.; Suib, S. L. Biosynthesis of Iron and Silver Nanoparticles at Room Temperature Using Aqueous Sorghum Bran Extracts. *Langmuir* **2011**, *27*, 264−271.

(11) Kaviya, S.; Santhanalakshmi, J.; Viswananthan, B.; Muthumary, J.; Srinivasan, K. Biosynthesis of silver nanoaprticles using citrus sinensis peel extract and its antibacterial activity. *Spectrochim. Acta A* **2011**, *79*, 594−598.

(12) Kumaravel, K.; Ravichandran, S.; Balasubramanian, T.; Sivasubramanian, K.; Bhat, B. A. Antimicrobial Effect of Five Seahorse Species From Indian Coast. *Br. J. Pharm. Toxicol.* **2010**, *1*, 62−66.

(13) Brewer, G. J. The Risks of Copper Toxicity Contributing to Cognitive Decline in the Aging Population and to Alzheimer's Disease. *J. Am. Coll. Nutr.* **2009**, *28*, 238−242.

(14) Mercado, J. J. R.; Reyes, E. R.; Lozano, M. A. Genotoxic effects of vanadium (VI) in human peripheral blood cells. *Toxicol. Lett.* **2003**, *144*, 359−369.

(15) Berradi, H.; Bertho, J. M.; Dudoignon, N.; Mazur, A.; Grandcolas, L.; Baudelin, C.; Grison, S.; Voision, P.; Gourmelon, P.; Dublineau, I. Renal Anemia Induced by Chronic Ingestion of Depleted Uranium in Rats. *Toxicol. Sci.* **2008**, *103*, 397−408.

(16) Chien, Y. H.; Huang, C. C.; Wang, S. W.; Yeh, C. S. Synthesis of nanoparticles: sunlight formation of gold nanodecahedra for ultra-sensitive lead-ion detection. *Green Chem.* **2011**, *13*, 1162−1166.

(17) Xu, X. Y.; Daniel, W. L.; Wei, W.; Mirkin, C. A. Colorimetric Cu^{2+} Detection Using DNA-Modified Gold-Nanoaprticle Aggregates as Probes and Click Chemistry. *Small* **2010**, *6*, 623−626.

(18) Lee, J. H.; Wang, Z.; Liu, J.; Lu, Y. Highly Sensitive and Selective Colorimetric Sensors for Uranyl (UO_2^{2+}): Development and Comparison of Labeled and Lable-Free DNAzyme- Gold Nanoparticle Systems. *J. Am. Chem. Soc.* **2008**, *130*, 14217−14226.

(19) Yin, J.; Wu, T.; Song, J.; Zhang, Q.; Liu, S.; Xu, R.; Duan, H. SERS-Active Nanoparticles for Sensitive and Selective Detection of Cadmium Ion (Cd^{2+}). *Chem. Mater.* **2011**, *23*, 4756−4764.

(20) Dang, Y. Q.; Li, H. W.; Wang, B.; Li, L.; Wu, Y. Selective Detection of Trace Cr^{3+} in Aqueous Solution by Using 5,5′-Dithiobis (2-Nitrobenzoic acid)- Modified Gold Nanoparticles. *ACS Appl. Mater. Interfaces* **2009**, *1*, 1533−1538.

(21) Chen, X.; Cheng, X.; Gooding, J. J. Multifunctional modified silver nanoparticles as ion and pH sensors in aqueous solution. *Analyst* **2012**, *137*, 2338−2343.

(22) Saha, K.; Agasti, S. S.; Kim, C.; Li, X.; Rotello, V. M. Gold Nanoparticles in Chemical and Biological Sensing. *Chem. Rev.* **2012**, *112*, 2739−2779.

(23) Sugunan, A.; Thanachayanont, C.; Dutta, J.; Hilborn, J. G. Heavy-metal ion sensors using chitosan-capped gold nanoparticles. *Sci. Technol. Adv. Mater* **2005**, *6*, 335−340.

(24) Tharmaraj, V.; Pitchumani, K. Alginate stabilized silver nanocube-Rh6G composite as a highly selective mercury sensor in aqueous solution. *Nanoscale* **2011**, *3*, 1166−1170.

(25) Chung, C. H.; Kim, J. H.; Jung, J.; Chung, B. H. Nuclease-resistant DNA aptamer on gold nanoparticles for the simultaneous detection of Pb^{2+} and Hg^{2+} in human serum. *Biosens. Bioelectron.* **2013**, *41*, 827−832.

(26) Cao, H.; Wei, M.; Chen, Z.; Huang, Y. Dithiocarbamate-capped silver nanoparticles as a resonance light scattering probe for simultaneous detection of lead(II) ions and cysteine. *Analyst* **2013**, *138*, 2420−2426.

(27) Hung, Y. L.; Hsiung, T. M.; Chen, Y. Y.; Huang, Y. F.; Huang, C. C. Colorimetric Detection of Heavy Metal Ions Using Label-Free Gold Nanoparticles and Alkanethiols. *J. Phys. Chem., C* **2010**, *114*, 16329−16334.

(28) Lin, Q.; Lin, J.; Lu, J.; Li, B. Biochemical Composition of Six Seahorse Species, Hippocampus sp., from the Chinese Coast. *J. World Aquaculture Soc.* **2008**, *39*, 225−234.

(29) Dubey, S. P.; Lahtinen, M.; Sarkka, H.; Sillanpaa, M. Bioprospective of *Sorbus aucuparia* leaf extract in development of silver and gold nanocolloids. *Colloids Surf. B: Biointerf.* **2010**, *80*, 26−33.

(30) Selvakannan, P. R.; Swani, A.; Srisathiyanarayanan, D.; Shirude, P. S.; Pasricha, R.; Mandale, A. B.; Sastry, M. Synthesis of Aqueous Au Core-Ag Shell Nanoparticles Using Tyrosine as a pH-Dependent Redusing agent and Assembling Phase-Transferred Silver Nano-particles at the Air-Water Interface. *Langmuir* **2004**, *20*, 7825−7836.

(31) Yilmaz, M.; Turkdemir, H.; Kilic, M. A.; Bayram, E.; Cicek, A.; Mete, A.; Ulug, B. Biosynthesis of silver nanoparticles using leaves of *stevia rebaudiana*. *Mater. Chem. Phys.* **2011**, *130*, 1195.

(32) Li, Y.; Qian, Z. J.; Kim, S. K. Cathepsin B inhibitory activities of three new phthalate derivatives isolated from seahorse, *Hippocampus Kuda* Bleeler. *Bioorg. Med. Chem. Lett.* **2008**, *18*, 6130−6134.

(33) Schmitt, J.; Machtle, P.; Eck, D.; Mohwald, H.; Helm, C. A. Preparation and Optical Properties of Colloidal Gold Monolayers. *Langmuir* **1999**, *15*, 3256−3266.

(34) Fayaz, A. M.; Girilal, M.; Venkatesan, R.; Kalaichelvan, P. T. Biosynthesis of anisotropic gold nanoparticles using *Maduca longifolia* extract and their potential in infrared absorption. *Colloids Surf. B: Biointerf.* **2011**, *88*, 287−291.

(35) Filippis, V. D.; Boni, S. D.; Dea, E. D.; Dalzoppo, D.; Grandi, C.; Fontana, A. Incorporation of the fluorescent amino acid 7-azatryptophan into the core domain 1−47 of hirudin as a probe of hirudin folding and thrombin recognition. *Protein Sci.* **2004**, *13*, 1489−1502.

(36) Chen, Y.; Rich, R. L.; Gai, F.; Petrich, J. W. Fluorescent Species of 7-Azaindole and 7-Azatryptophan in water. *J. Phys. Chem.* **1993**, *97*, 1770−1780.
(37) Sariciftci, N. S.; Smilowitz, L.; Heeger, A. J.; Wudl, F. Photoinduced Electron Transfer from a Conducting Polymer to Buckminsterfullerene. *Science* **1992**, *258*, 1474−1476.
(38) Pattison, D. I.; Rahmanto, A. S.; Davies, M. J. Photo-oxidation of Proteins. *Photochem. Photobiol. Sci.* **2012**, *11*, 38−53.
(39) Kreibig, U.; Althott, A.; Pressman, H. Veiling of Optical Single Particle Properties in Many Particle Systems by Effective Medium and Clustering Effects. *Surf. Sci.* **1981**, *106*, 308−317.
(40) Quinten, M.; Kreibig, U. Optical Properties of Aggregates of Small Metal Particles. *Surf. Sci.* **1986**, *172*, 557−577.
(41) Xu, D.; Tsai, C. J.; Nussinov, R. Hydrogen bonds and salt bridges across protein-protein interfaces. *Protein Eng.* **1997**, *10*, 999−1012.
(42) Guarise, C.; Pasquato, L.; Scrimin, P. Reversible Aggregation/Deaggregation of Gold Nanoparticles Induced by a Cleavable Dithiol Linker. *Langmuir* **2005**, *21*, 5537−5541.
(43) Liu, Z.; Jiang, M. Reversible aggregation of gold nanoparticle driven by inclusion complexation. *J. Mater.Chem.* **2007**, *17*, 4249−4254.
(44) Si, S.; Mandal, T. K. pH-Controlled Reversible Assembly of Peptide-Functionalized Gold Nanoparticles. *Langmuir* **2007**, *23*, 190−195.
(45) Zhu, M. Q.; Wang, L. Q.; Exarhos, G. J.; Li, A. D. Q. Thermosensitive Gold Nanoparticles. *J. Am. Chem. Soc.* **2004**, *126*, 2656−2657.
(46) Sun, L.; Zhao, D.; Ding, M.; Xu, Z.; Zhang, Z.; Li, B.; Shen, D. Controllable Synthesis of Silver Nanoparticle Aggregates for Surface-Enhanced Raman Scattering Studies. *J. Phys. Chem. C* **2011**, *115*, 16295−16304.
(47) Merlen, A. Surface-Enhanced Raman and Fluorescence Spectroscopy of Dye Molecules Deposited on Nanostructured God Surfaces. *J. Phys. Chem. C* **2010**, *114*, 12878−12884.
(48) Galopin, E.; Barbillat, J.; Coffinier, Y.; Szunerits, S.; Patriarche, G.; Boukherroub, R. Silicon Nanowires Coated with Silver Nanostructures as Ultrasensitive Interfaces for Surface-Enhanced Raman Spectroscopy. *ACS Appl. Mater. Interfaces* **2009**, *1*, 1396−1403.
(49) Ruan, C.; Wang, W.; Gu, B. Single-molecule detection of thionine on aggregated gold nanoaprticles by surface enhanced Raman scattering. *J. Raman Spectrosc.* **2007**, *38*, 568−573.
(50) Watanable, H.; Hayazawa, N.; Inouye, Y.; Kawata, S. DFT Vibrational Calculations of Rhodamine 6G Adsorbed on Silver: Analysis of Tip-Enhanced Raman Spectroscopy. *J. Phys. Chem. B* **2005**, *109*, 5012−5020.